INTERNAL REPORT

SRT Site Monitoring: A comparison between GPS and Radiosonde data

Francesco Nasir, Franco Buffa, and Gian Luigi Deiana

Report N. 22, released: 20/10/2012

Reviewer: Ignazio Porceddu

OAC Osservatorio Astronomico di Cagliari

Abstract

The Sardinia Radio Telescope (SRT) is a challenging scientific project managed by the National Institute for Astrophysics (INAF), the radiotelescope site is at 30 km North of the city of Cagliari (Italy). The goal of the SRT project is to build the most powerful Italian radio telescope consisting of a general purpose, fully steerable, 64 m diameter radio telescope, capable of operating with high efficiency in a wide frequency range (0.3-100 GHz). The SRT can be operated in single dish mode or combined with other radio telescopes as part of the existing Very Long Base Line Interferometry (VLBI) network.
Extraterrestrial radio signals are very weak, therefore atmospheric conditions have a great influence on SRT's capability to perform good measurements. This is the reason why the SRT will need a reliable atmospheric monitoring system. A state of the art radiometer operating in K and V spectral bands has been acquired to monitor the SRT atmosphere, as well as a geodetic GPS receiver capable of retriving integrated water vapor. These instruments will provide real time measurements of atmospheric parameters useful for scheduling astrophysical observations when the atmospheric conditions are suitable for the project.
Furthermore, the Astronomical Observatory of Cagliari (OAC) has obtained a 50-years dataset (1950-2007) of radiosonde launches conducted between 1950 and 2007 by several radiosonde experiments at the airport of Cagliari. Through radiosonde measurements and an appropriate radiative transfer model, we have performed a statistical analysis of the SRT atmosphere that accounts for opacity at different frequencies, water vapor and cloud liquid, mean profiles of relative humidity, mean temperature and wind. This climatic analysis will be useful for scheduling astronomical observations at different frequencies in the most appropriate time frame during the year.
The results show that at frequencies lower than 20 GHz, water vapor and weather conditions have little or no influence on the quality of astronomical observations. Water vapor has instead a big effect on the quality of 22 GHz observations with the winter months being considerably more indicated than summer ones. Integrated water vapor content at the SRT site during winter ranges, on average, between 7 and 15 mm. Our statistical study indicates that observations at high frequencies between, 50 GHz and 100 GHz, may be feasible during winter months.

1 Introduction

The Sardinia Radio Telescope (SRT) is a project by the Italian National Institute for Astrophysics (INAF) in an advanced stage of realization in Sardinia (http://www.srt.inaf.it). Its precise location is called "Pranu Sanguni", close to the town of San Basilio (Lat. 39°29'50"N - Long. 09°14'40"E, Alt. 630 m) at 30 km North of Cagliari. It is a 64 m diameter, fully steerable, radiotelescope with AltAz mount and high versatility that allows for different focal positions and a wide frequency range (0.3 to 100 GHz). Furthermore, the SRT can be used in single-dish mode and it can also function with VLBI networks in order to achieve angular resolution of the order of milliarcseconds. The SRT, designed for radio astronomy, geodynamics and space sciences, will certainly become an important and high profile instrument in the European scenario.
It is understood that one of the limiting factors for radio-astronomical observations, thus for SRT observations is given by the states of the atmospheric constituents, in particular, the atmospheric water vapor content, which can vary rapidly in space and in time (Memmo et al., 2005). Water vapor is a great absorber at microwave frequencies, hence it can reduce the intensity of radio-astronomical signals. In particular observations at high frequencies (20-100 GHz) need to be made during excellent weather conditions. This is the reason why we have firstly conducted a climatic statistical study by analysing a 50-years dataset of radiosondes, launched periodically at Cagliari airport at roughly 30 km from the SRT, which measure relative humidity, temperature, pressure and wind profiles. Through these quantities and the use of an appropriate radiative transfer model we have simulated atmospheric brightness temperatures and opacities at frequencies tipically observed by radio telescopes. In addition, we conducted a statistical study on integrated water vapor, liquid content and winds. This analysis is complementary to our real time weather monitoring system comprised of a radiometer, a geodetic GPS receiver and a ground based meteorological station. The investigation of the radiosonde dataset, together with the outcome of the aforementioned instruments will help us investigate in which period of the year and of the day astronomical observations at different frequencies should be performed preferably. As for this report, we focus on the climatic analysis through the radiosonde dataset. In future work we will report on the radiometer and the geodetic GPS real time measurements of geophysical quantities and nowcasting.
This report should be considered as the continuation of the works by Sandri and Ambrosini (1999) and Pacione et al. (2002). It is structured as follows: in section 2 we discuss the SRT's scientific aims with particular attention to the frequencies that will be used for the observations, in section 3 the observed geophysical quantities are discussed. Section 4 describes the radiosonde dataset and the radiative transfer model used to simulate the atmospheric absorption. In section 5 we discuss the results of the water vapor and cloud liquid content, wind and especially opacity statistics, then in section 6 we wrap up the report and discuss results and future work. Finally, in appendix A and B, monthly and seasonal cumulative distribution functions of IWV and opacity at different frequencies are presented respectively.

2 Scientific aims of SRT

This section provides an overview of the main scientific topics that can be investigated through observations with the SRT in "single-dish" and "VLBI" mode (further details are found at "http//www.srt.inaf.it/science"). Furthermore, we also discuss the main frequencies at which the SRT will observe. Radio observations aim mostly at detecting continuum and/or line emission from galactic and extragalactic objects. The former emission is produced in a continuous range of frequencies, throughout all the radio band, by three main physical processes: synchrotron, bremsstrahlung and inverse Compton. Main galactic targets of this type of observations are: pulsars (especially at lower frequencies, <5 GHz), supernova remnants and HII regions. Extragalactic sources tipically studied comprise AGN and clusters of galaxies.
Concerning spectral line studies, the SRT will offer unique tuning capabilities between different frequencies because of its agility in receiver switching. The three first light receivers will be those at

L & P (dual frequency receiver), C and K band. At low frequencies (0.3-1.4 GHz), observations of local and redshifted neutral hydrogen, the most abundant atomic element in space, will be performed. Around 6.7 GHz, methanol (CH_3OH) maser studies from galactic massive star forming regions will unveil the dynamics of the gas around these young stellar objects, tipically obscured at optical wavelenghts.
Moving up to higher frequencies, we encounter the 22 GHz band, where we find the well known main maser transition of the water molecule at 22.23 GHz. The characteristics of this emission (e.g. strength and compactness) allows detailed studies of outflowing gas in galactic star forming regions and in the case of the extremely luminous extragalactic H_2O megamasers, VLBI mapping of accretion disks and black hole mass estimates. Noticeably, the 22 GHz frequency is highly absorbed because it corresponds to the resonant absorption line of water vapor in the atmosphere. Therefore, weather conditions and, in particular, the water vapor content have a strong effect on the quality of these observations, strengthening the importance of our studies of atmospheric conditions at the SRT site.
The next generation of receivers planned to be installed on the SRT will cover also higher frequencies, from the K band to about 100 GHz. In this frequency range many relevant line transitions are observable. Among these, the silicon monoxide (SiO) thermal and maser emission (at $\sim$ 40 GHz) and the hydrogen cyanide (HCN) and hydrogen isocyanide (HNC) lines (at $\sim$ 90 GHz), that are particularly important tracers of high-density gas.
Last but not least, we have to mention the carbon monoxide CO main transitions (at $\sim$ 110 GHz). They are produced by non elastic collisions between CO and H_2 molecules. The latter is the most abundant molecular specie in space but, oddly, can not be observed directly in the cold molecular clouds of the interstellar medium. Hence, CO observations provide us with an indirect way to infer the distribution and physical conditions of H_2 both in the galactic medium and in the environment of starburst galaxies.
Needless to say that in order to perform observations with the SRT at such high frequencies, excellent weather conditions are mandatory. The study described in this report and the following works planned by our group are indeed aimed at determining the percentage of time at which the SRT will be able to perform good observations at the aforementioned ranges of frequencies.

3 Geophysical Quantities

In this report we will deal mainly with water vapour and cloud liquid water content, atmospheric opacity and tropospheric delays, therefore it may be useful to give a short description of these quantities.

Water vapour content, which is often referred to as precipitable water vapour PWV or integrated water vapour IWV, is the height of the column of water per unit surface that would be obtained if all the vapour in a particular direction in the sky were to condense (for simplicity from now onwards we will consider only the zenith direction). It is measured in kg/m^2 or equivalently in mm, its expression is the following (Janssen, 1992):

$$IWV = \int_0^\infty SH(z)dz; \tag{1}$$

where SH is the specific humidity measured in kg/m^3 and it can be expressed through the ideal gas equation:

$$SH(z) = \frac{e}{R_v T}. \tag{2}$$

where R_v is the water vapor gas constant, $T(z)$ is temperature and $e(z)$ is water vapour partial pressure at a given height for a given relative humidity and temperature value. The latter can be deduced by means of the Clausius Claypeiron equation, in fact if relative humidity RH and temperature profiles are known we can write:

$$e(z) = RH(z) \cdot e(z_0) exp[\frac{L_v}{R_v}(\frac{1}{T(z_0)} - \frac{1}{T(z)})], \tag{3}$$

where $L_v = 2.5 \cdot 10^6\ J/kg$ is water's latent heat of vaporization. By using equations 3 and 2 and integrating numerically equation 1 it is possible to evaluate IWV from the radiosonde profiles. The quality of radio-astronomical observations depends greatly on IWV, this is why great attention is focussed on this quantity.

Integrated liquid water ILW is the height of the column of water per unit surface that would be obtained by taking into account all the cloud liquid water in a particular direction in the sky, it is measured in kg/m^2 or equivalently in mm its expression is the following (Turner et al., 2007):

$$ILW = \int_{H_{inf}}^{H_{sup}} LWC(z)dz; \tag{4}$$

where H is cloud height and LWC is liquid water content measured in kg/m^3, it can be expressed as:

$$LWC(z) = \frac{4}{3}\pi\rho_l \int_{r_{min}}^{r_{max}} r^3 n(r)dr; \tag{5}$$

where ρ_l is liquid water density, r is water droplet radius and $n(r)$ is the size distribution per unit volume of water droplets inside a cloud. Absorption by cloud liquid water is important although it is usually less than that of water vapor content, more details on this topic are given at the end of section 5.2.

The relationship that links atmospheric constituents (gases and hydrometeors) to radiative emission or absorption is given by the radiative transfer equation RTE (Janssen, 1992). For microwave emission we can use the Raleigh-Jeans approximation, in this case radiative emission is expressed in terms of brightness temperature T_b as:

$$T_b(\nu) = T_c e^{-\tau_\nu(0,\infty)} + \int_0^\infty \alpha_\nu(z) T(z) e^{-\int_0^z \alpha_\nu(z')dz'} dz; \tag{6}$$

where α_ν is the absorption coefficient at a given frequency ν expressed in Np/m, T is the physical temperature, T_c is the cosmic background temperature and

$$\tau_\nu = \int_0^\infty \alpha_\nu(z)dz \tag{7}$$

is the atmospheric opacity (integrated atmospheric absorption) evaluated along the path z. Equation 6 is valid if scattering by water and ice particles can be neglected, this is usually true for frequencies such as 22 GHz although approaching 100 GHz, heavy rainfall and hail may cause non negligible scattering contributions (Petty, 2006).
The RTE is often referred to as a Fredholm integral equation of the first kind. If T_b values at different frequencies are known than it is possible to retrive information on atmospheric constituents indirectly through the absorption coefficient. The techniques used to invert the RTE depend on the geophysical quantities that one wants to retrive. In general it is important to note that equation 6 yields two cases:

- *direct problem*: given a set of atmospheric radiosonde profiles (e.g. relative humidity, temperature, pressure and liquid water content) one wants to evaluate atmospheric emission and/or absorption. This is what we did in this report by using the airport radiosonde dataset and the radiative transfer model ARTS.

- *indirect problem*: given a set of radiative measurements (e.g. radiometer T_b measurements) we want to retrive atmospheric profiles such as temperature and relative humidity ones and/or integrated quantities such as IWV and ILW. The indirect problem is by far the most complicated because it can be ill-posed: more than one combination of atmospheric profiles may correspond to the set of radiative measurements. To remove this ambiguity we must impose constraints on the problem at hand.

Recently OAC has aquired a microwave radiometer mainly to monitor IWV and ILW contents at the SRT site. Radiometer channels corresponds to different frequencies, which in turn may unveil information on a given gas specie that absorbs and emits at that particular frequency. For example, water vapour's resonant frequency $\nu_1 = 22.23\ GHz$ is useful to gain information on integrated water vapour IWV. On the other hand $\nu_2 = 31.1\ GHz$ is not a resonant frequency for any gas specie so its emission depends mainly on integrated cloud liquid water ILW. By choosing with care two non ambiguous frequencies such as the ones just mentioned and neglecting scattering it is possible to obtain the following set of linear equations starting from the RTE:

$$\tau(22) = \tau_{O_2}(22) + K_L(22) \cdot ILW + K_V(22) \cdot IWV \tag{8}$$

$$\tau(31) = \tau_{O_2}(31) + K_L(31) \cdot ILW + K_V(31) \cdot IWV \tag{9}$$

where τ_{O_2} is the opacity of oxygen and K_L and K_V are the absorption coefficient per unit density respectively of liquid water and of water vapour. These quantities are found in literature or can be deduced from climatological data, so we can solve for two unknowns ILW and IWV.
Opacity τ can be obtained with radiometric measurements too through the following equations (Wu, 1979):

$$\tau_\nu = ln[\frac{(T_{mr}(\nu) - T_c)}{(T_{mr}(\nu) - T_b(\nu))}]; \tag{10}$$

where

$$T_{mr} = \frac{\int_0^\infty \alpha(z)T(z)e^{-\tau(0,z)}dz}{\int_0^\infty \alpha(z)e^{-\tau(0,z)}dz}; \tag{11}$$

is the mean radiative temperature. We used radiosonde profiles and ARTS to recover an empirical relationship between surface temperature and T_{mr}, this will be useful in future to measure opacity at the SRT site with the new radiometer.

Previously we illustrated how a basic bi-frequency radiometer can retrive liquid water and vapour and opacity. By using a multi-frequency channel radiometer and more sophisticated retriving techniques its possible to obtain not just integrated quantities but also vapour and temperature profiles.

As mentioned before, a geodetic GPS receiver has been installed at the SRT site, such instruments can measure IWV indirectly by measuring the excess of optical path due to refractivity in the zenithal direction. Usually zenith tropospheric delay ZTD, is subdivided in the hydrostatic component ZHD and in the wet component ZWD (Bevis et al., 1996):

$$ZTD = ZHD + ZWD = 10^{-6} \int_s N ds \tag{12}$$

where $N = 10^6(n-1)$ represents refractivity and n is the refraction index. The hydrostatic component is given by the next equation:

$$ZHD = 10^{-6} k_1 \int_s \frac{P_h}{T} ds \tag{13}$$

where P_h is the partial pressure of dry air. The wet component of the tropospheric delay (Mendez et al., 2000) is given by:

$$ZWD = 10^{-6}(k_2 + \frac{k_3}{T_m}) \int_s \frac{P_w}{T} ds; \tag{14}$$

where k_1, k_2 and k_3 are refractivity constants, P_w is the water vapour partial pressure and

$$T_m = \frac{\int_s \frac{P_w}{T} ds}{\int_s \frac{P_w}{T^2} ds}, \tag{15}$$

is the mean atmospheric temperature. As in the case of T_{mr} we used the historical radiosonde data set to recover an empirical relationship between surface temperature and T_m.
Integrated water vapour IWV is related to ZWD through the following relationship:

$$ZWD = \Pi \cdot IWV; \tag{16}$$

where

$$\Pi = 10^{-6}(k_2 + \frac{k_3}{T_m})R; \tag{17}$$

and R is the universal constant of gasses. As mentioned before geodetic GPS can measure ZTD, to find ZWD we must measure ZHD and T_m independently, this can be done with good approximation with empirical models taken from literature and a ground meteorological station positioned close to the geodetic GPS receiver.

In future we will have radiometer water vapour and liquid retrivals at the SRT site together with GPS water vapour measurements. These will increase our knowledge on the SRT site's atmosphere and in time they will contribute to the creation of a robust data set. In addition to this, geophysical measurements will be useful for scheduling astrophysical observations in real time and they could contribute to implementing a nowcasting system: a system based on statistical methods that forecasts vapour and cloud liquid for a short period ahead.

In this report the priority is given to the historical data set of radiosonde profiles launched at Cagliari airport. With this dataset we have conducted a climatic statistical study of the SRT site's atmosphere focusing particularly on its emission and its absorption characteristics during the year. To do this we used a radiative transfer model to simulate emission by resolving the direct problem. This wide dataset was also useful to find empirical models for T_{mr} necessary to evaluate opacity with radiometric measurements and T_m necessary to evaluate IWV with GPS tropospheric delay measurements, more details are given in the following section.

4 Radiosonde Analysis and Radiative Transfer Model

In atmospheric sciences, radiosondes are usually considered the reference instrument for all the other techniques (Cimini et al., 2009), during their ascent a radiosonde measures pressure, temperature, wind and relative humidity directly. These observations together with the sonde's position, measured with an on-board GPS receiver, are transmitted with continuity to a ground receiver. These measurements can be used to model atmospheric temperature and water vapour vertical distribution and to estimate brightness temperature and opacity at different frequencies through a radiative transfer model. On the other hand radiosondes are by no means perfect instruments, providing a limited number of observations. For a given location they are launched only 2 to 4 times a day and their sensors are often characterized by systematic errors (Cimini et al., 2009).
The radiosonde dataset was acquired from the Italian Air Force, which has an operative base at Cagliari airport (LIEE) since 1950, this is the closest radiosonde launch site to the SRT. The dataset ranges from 1950 to 2007 and it corresponds mainly to 00 and 12 UTC. In addition to this we have a denser but smaller timeseries of radiosonde measurements performed at Cagliari airport that ranges from 1998 to 2000 with high daily launch frequency (4 times a day).
The raw radiosonde measurements were acquired in a specific airforce format (TEMP) and they are often contaminated by recording errors or missing information which makes some of the datafiles useless. Thus a pre-filtering process was necessary to "clean up" and organize observations in data structures as illustrated in table 1. Although the dataset ranges from 1950 to 2007 the pre-filtering

Data structure: mdata	**Description**
mdata.anno	int
mdata.mese	int
mdata.giorno	int
mdata.ora	int
mdata.PW	float, [mm], precipitable water at station level
mdata.isok	boolean, false if data is missing or corrupt
mdata.P(i)	float, [hPa], pressure
mdata.z(i)	float, [m], height
mdata.T(i)	float, [°C], temperature
mdata.D(i)	float, [°C], dew point temperature
mdata.H(i)	int, [%], relative humidity

Table 1: Data structure used for radiosonde measurements archive.

process reduced the historical data set to roughly 25 years of observations (1980-2007), nevertheless this allows us to deduce climatic patterns and mean atmospheric values at the SRT site.

We also considered absorption and emission contributions by cloud liquid on millimeter wavelengths and conducted statistics in terms of liquid water content LWC, integrated liquid water ILW and cloud cover frequency during the year. LWC was fed into the radiative transfer model in order to simulate more precisely the emission and absorption properties of the SRT site's atmosphere. Unfortunately radiosondes do not measure LWC directly so we used an empirical model calibrated on the Mediterranean region (Pulvirenti et al., 2005) to evaluate this quantity, more details will be given in section 5.2.

The radiative transfer model used was ARTS (Atmospheric Radiative Transfer Simulator) version 1.0.214, this code is particularly useful for millimeter and submillimeter wavelenghts (Buehler et al., 2005). ARTS simulates the radiation that a passive remote sensing instrument would receive from the atmospheric gas components and it carries out scalar calculations, which means that it treats only the first component of the Stoke's vector. Calculations are performed under precise atmospheric conditions defined by geophysical profile inputs such as temperature, pressure, relative humidity and

liquid water content profiles. The primary vertical coordinate is pressure, all other quantities such as geometric altitude and trace gas concentrations, are given on pressure grids. The model can be used to simulate measurements for any observation geometry: up looking, down looking, or limb looking, and for any sensor position: on the ground, inside the atmosphere, or on a satellite. It works with arbitrary frequency grids, hence it can be used both for the simulation of high resolution sensors, and for the simulation of broad frequency ranges. The applicable spectral range is from the microwave up to the thermal infrared. In that frequency range, particular care has been taken to make the absorption calculation consistent with state of the art continuum models for water vapor and nitrogen, and with continuum and line mixing models for oxygen. The ARTS version we used doesn't take into account scattering by large water droplets or ice particles although for non precipitating clouds and frequencies below 100 GHz scattering doesn't contribute significantly to the overall emission (Cimini et al., 2007).
In order to use ARTS its necessary to write a control file that loads a set of geophysical profiles in ARTS format so that they can be fed to the executable programme. Furthermore in the control file the observing geometry must be specified together with the vertical pressure spacing, the instrument platform altitude, the frequency grid, the atmospheric absorption models for each atmospheric constituent, the zenith angle and other less important features. For a large radiosonde profile dataset it was necessary to automatize this procedure. This was done by using OCTAVE programming language (http://www.gnu.org/software/octave), furthermore OCTAVE was also used to perform statistics, plots and other calculations, these drivers are available at "http://laser3.ca.astro.it".

Considerations must also be made on the fact that the radiosonde launches were performed 30 km away from the radiosonde site and at a different altitude. The SRT is located on an inland plateau at 630 m of altitude and it is relatively distant from the sea. The radiosonde launch location is at sea level at a few km from the Gulf of Cagliari and at a few hundred m from the Santa Gilla lagoon. During its vertical ascent a radiosonde may move horizontally by as much as 20 to 40 km as will be

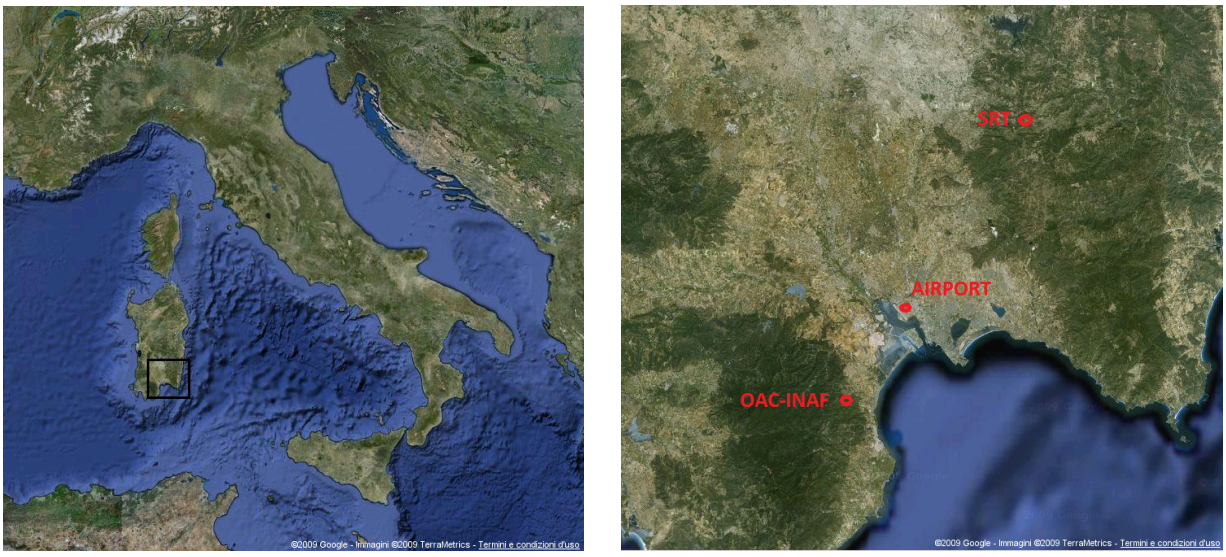

(a) (b)

Figure 1: SRT, OAC and Cagliari airport site.

shown in the following sections, so in actuality a radiosonde profile is not rigourously a vertical one. For this reason and also because atmospheric horizontal gradients vary slowly (Holton, 2004) it is safe to assume that radiosonde measurements performed at Cagliari airport are quite representative of the SRT site's atmosphere. Nevertheless the airport's lower atmosphere's microclimate is probably characterized by deep convection and turbulent mixing due to intense moisture and heat exchanges

between sea, land and the lagoon. As height increases, especially above the boundary layer, the climatological differences between the two sites should decrease. This is why care had to be taken when using the radiosonde dataset: although the SRT site is at a higher altitude than the radiosonde launch location, we are skeptic of simply clipping off the first 630 m of radiosonde measurements. In the analysis that follows we will illustrate always the "clipped case" and the "non-clipped" one together and we will assume that the right values are intermediate ones.

5 Results

In this section we will show statistics of integrated water vapor, cloud liquid and opacity (total atmospheric absorption) at several frequencies that correspond to those most likely to be used for SRT observations. Furthermore we will illustrate empirical relationships that have been obtained from the historical radiosonde dataset for mean temperature T_m and mean radiative temperature T_{mr} which in future will be useful to retrive respectively IWV through geodetic GPS tropospheric delay measurements and opacity through radiometer T_b measurements. Finally we will show mean relative humidity profiles and we will also show winds analysis.
The next section shows a comparison between GPS IWV taken at the SRT site and radiosonde IWV measurements taken at the airport.

5.1 Comparing GPS IWV measurements with Radiosonde ones

The SRT site is roughly at 30 km from the radiosonde launch site at Cagliari airport, nevertheless these measurements can be considered representative of the SRT site's atmosphere because horizontal temperature, pressure and relative humidity gradients vary quite slowly (Holton, 2004). In addition to this during its ascent through the troposphere a radiosonde can move horizontally by more than 20 km therefore radiosonde measurements are not strictly vertical.
To demonstrate that the atmosphere over the SRT site and over the airport are consistent with each other we took roughly 2 years (2007-2009) of radiosonde launches at Cagliari airport and evaluated IWV by using equations 3 and 2. Than we took IWV measurements at the SRT site made with a geodetic GPS that has been there since 2007, finally we compared the two sets of measurements. This gave us the chance to show firstly that the radiosonde measurements taken at Cagliari airport are representative of SRT's atmosphere, and this is important especially for the analysis that follows in the next sections.
In figure 2 we compare GPS IWV with radiosonde IWV, measurements correspond to 00 UTC and 12 UTC. As can be seen in figure 2, IWV content measured at the airport is systematically greater than

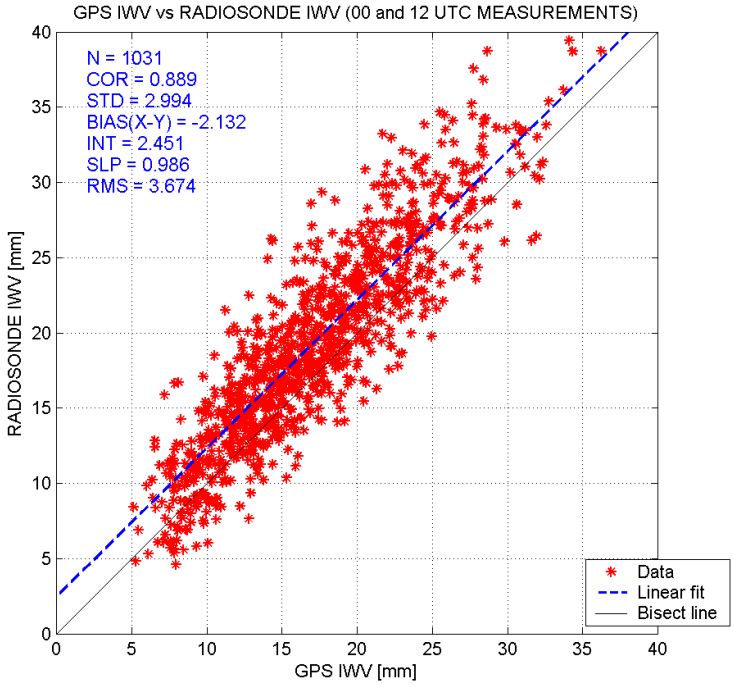

Figure 2: Radiosonde measured IWV (Cagliari airport) Vs geodetic GPS measured IWV (SRT site) in the period 2007-2009.

that measured at the SRT site by roughly 2 mm. At the same time data values are well aligned and correlated (correlation coefficient $\rho = 0.9$). Figure 2 tells us that it's quite safe to base our climatic analysis of the SRT atmosphere on historical datasets of radiosonde profiles launched at Cagliari airport.
Figure 2 shows night and day measurements together: by separating 00 UTC measurements from 12 UTC ones (fig. 3), we found out something interesting: during the night time IWV content at the airport is significantly greater than during the day time. Figure 3 shows that 00 UTC data points are

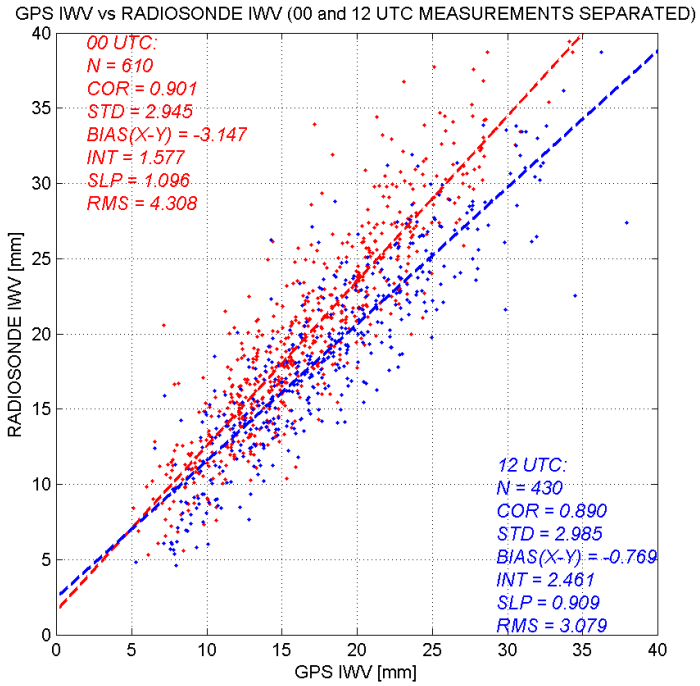

Figure 3: Radiosonde measured IWV (Cagliari airport) Vs geodetic GPS measured IWV (SRT site) at 00 UTC (red points) and 12 UTC (blue points) in the period 2007-2009.

more biassed (bias = 3.1) than 12 UTC ones (bias = 0.8). According to Clausius Claypeiron's equation (eq. 3) one would expect the opposite because during day time it is usually warmer. Nevertheless all the statistics that follow have been processed with respect to sea level and to SRT's altitude, this has shown that by cutting off lower altitudes the effect illustrated in figure 3 is weaker. In other words we think that the night time effect is due to boundary layer turbulent mixing and higher sea-air heat and vapor exchanges during the night time. In sections 5.2 and especially in section 5.5 we will carry on investigating this aspect.

5.2 Water Vapour and Cloud Liquid

In figure 4 we show IWV daily average values during a whole year separating night from day time at different altitudes (0 m and 630 m), the average has been obtained considering a 50-year dataset. The reason why we always show statistics for both the radiosonde launch altitude and the SRT altitude is because we are skeptic of simply clipping off the initial 630 m of radiosonde profiles: boundary layer effects, turbulent mixing and evapotranspiration make it difficult to simply assume that the SRT is free from all the water vapour below 630 m of altitude. So we reasonably believe that roughly the true value of IWV is somewhere in between: in the best case scenario it will be that corresponding to 630 m of altitude. In figure 4 one can see a typical IWV pattern in the South Sardinian region: at sea

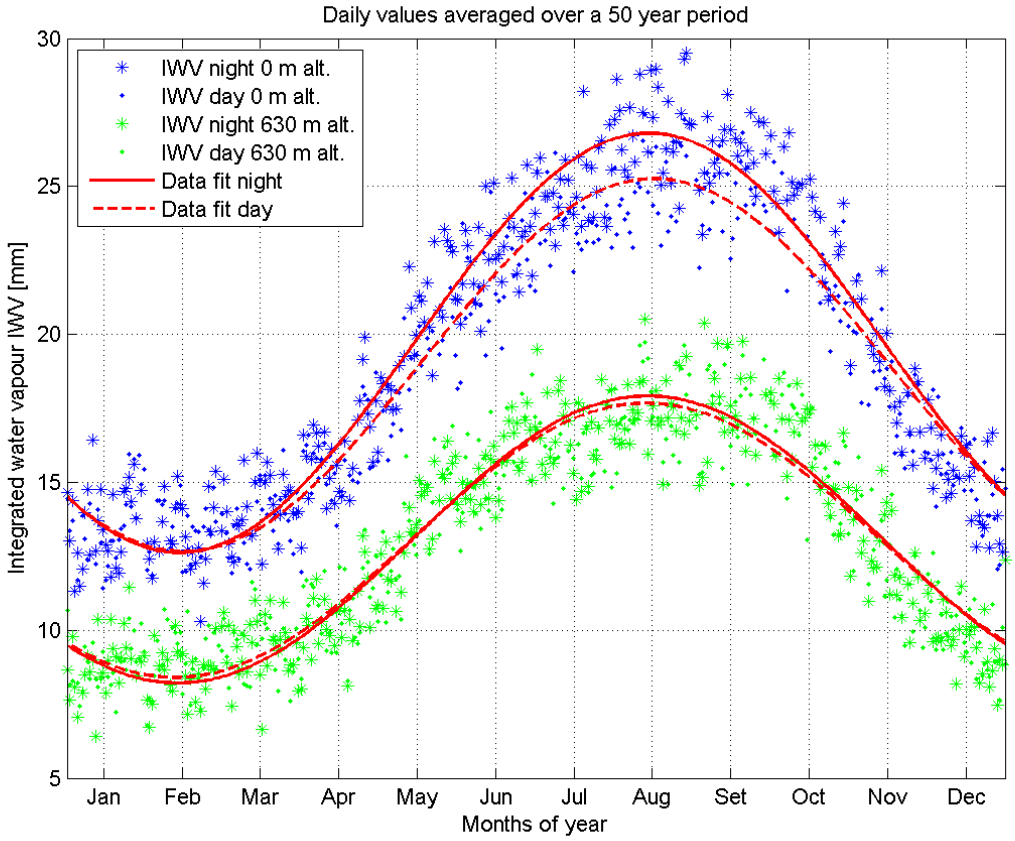

Figure 4: Radiosonde measured IWV at Calgiari airport separating night from day at different altitudes.

level IWV varies on average from 12 to 26 mm, in the summer water vapour is obviously much higher than in the winter time, thus making winter a better period for delicate astrophysical observations. At 630 m of altitude water vapour is lower than at sea level, there are several winter months in which $IWV < 10$ mm. Figure 4 also shows that at higher altitudes the night and day differences tend to disappear and this is an indication that this phenomenon is a boundary layer effect and it seems to be more intense during summer months than during winter ones.
Water vapour statistics can be shown in a more convenient way through cumulative distribution functions (CDF) which show the probability, for a given epoch, of finding a quantity (eg. IWV) below a certain value. Figure 5 shows seasonal CDF for IWV, we can see that during the winter and Spring there is more probability of encountering low IWV conditions while during the Summer and the Autumn IWV values are usually larger. Night and day differences are less visible at higher altitudes and during Winter months. Regarding astrophysical observations, it is interesting to see that during Winter months IWV is lower than 10 mm almost 50 % of the time, so for H_2O maser observations

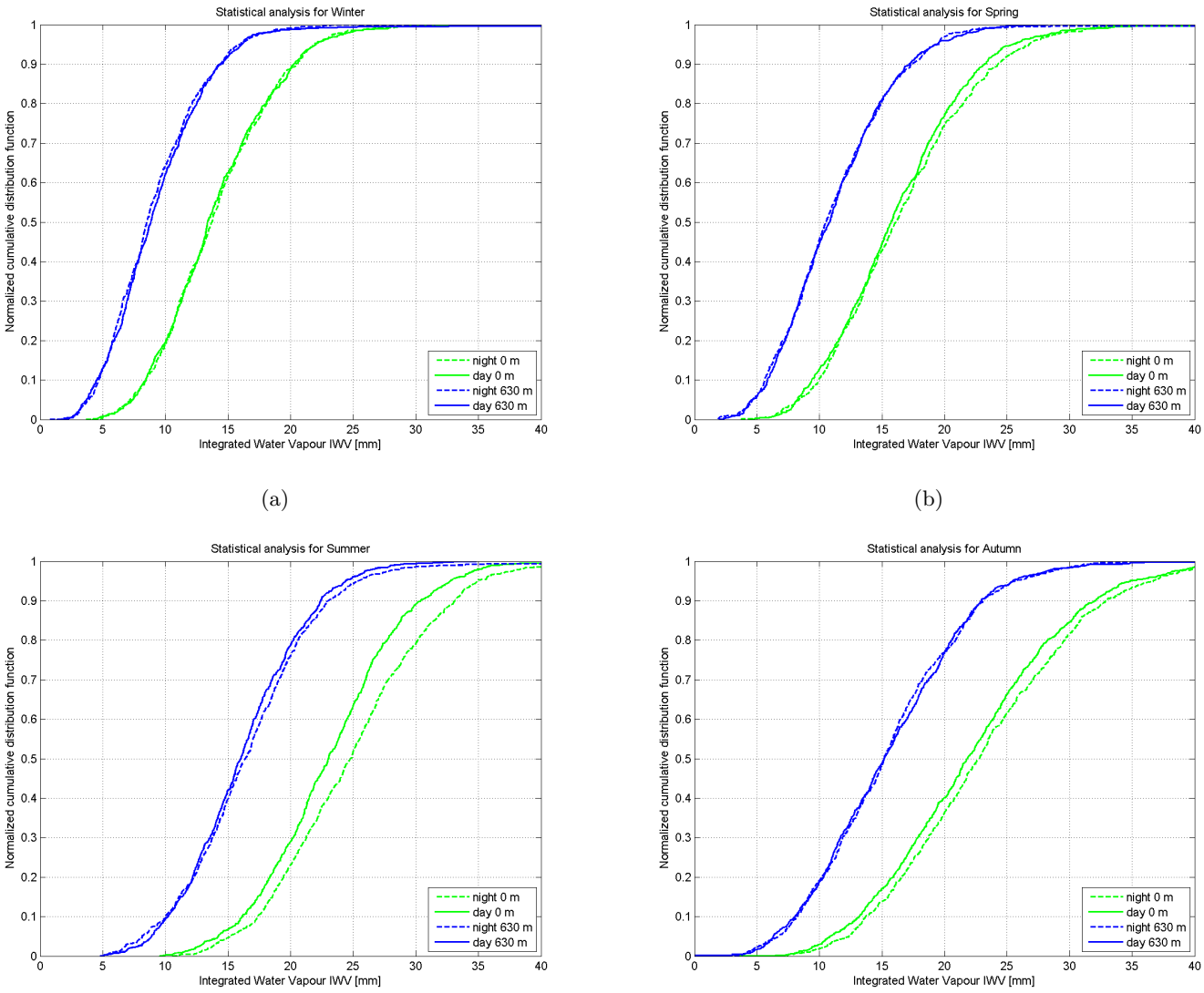

Figure 5: Seasonal IWV cumulative distribution functions.

and especially higher frequency observations such as CO emissions, there are a lot of days in which observations are possible.
In Appendix A it is possible to find the same type of plots as in figure 5 for all months of the year.

Besides water vapour, we also conducted statistics on liquid water vertical profiles LWC and integrated liquid water ILW. In actuality liquid water profiles can not be measured with radiosondes, nevertheless in literature there are several empirical models that can evaluate LWC by using as input radiosonde temperature, pressure and relative humidity profiles. We used an empirical model calibrated on the Mediterranean region (Pulvirenti et al., 2005), this model evaluates layer by layer a flexible critical relative humidity RH_c as a function of pressure. If the actual relative humidity is greater than RH_c than, according to the model, liquid formation at that hight is possible. The model then determines the amount of LWC as a function temperature, to estimate ILW we simply integrated LWC according to equation 4. To improve the model's LWC retrivals with respect to our location we optimized the parameters on which it depends through a simulated-annealing Monte Carlo scheme (Kirkpatrick et al., 1983).

In figure 6a we show ILW during the year obtained from the 50-years radisonde dataset, while in figure 6b we show the cloud cover probability for each month of the year. As we can see from the plots in

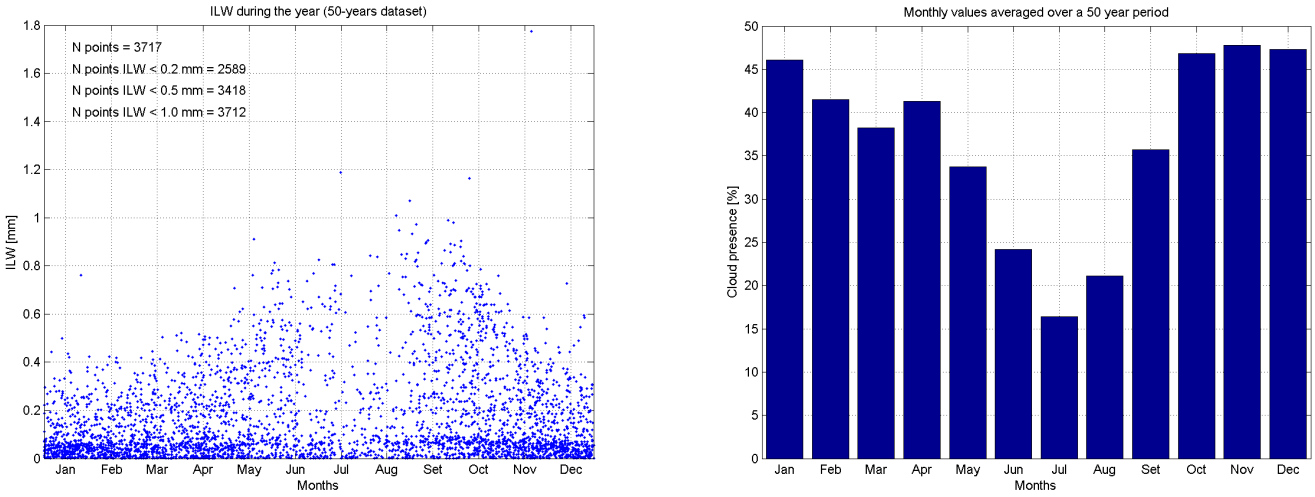

(a) (b)

Figure 6: (a) Daily averaged values of ILW, (b) average cloud presence during each month.

figure 6, typical values of ILW at the SRT site vary during the year from 0-0.2 mm during the Winter to 0-0.8 mm during the Summer. Nevertheless, during the Winter, cloud coverage is more probable than during the Summer, in fact the most cloudy month is November (cloud cover: 47% of the time) while the least cloudy is July (cloud cover: 16% of the time).
Although ILW values are small when compared with IWV ones, liquid water is important too in atmospheric emission processes, especially for window channels such as the 30 to 40 GHz ones. To better understand the effect of cloud liquid on radiative transfer processes at different frequencies we took radiosonde profiles that corresponded only to cloudy conditions. Furthermore we simulated opacity with ARTS by including liquid water and compared it with the opacity obtained without including liquid water, the difference between the simulations (fig. 7) is indicative of the weight that cloud liquid has on radiative processes at these frequencies. Figure 7 shows that at resonant frequencies such as 22.23 GHz the effect of cloud liquid is important but not comparable to the water vapor contribute: if clear sky opacity is 0.07 Np than liquid can contribute at the most by 0.01 Np: 12% of the total amount. For "window channels" such as 30 GHz liquid water is more important: if clear sky opacity is 0.07 Np than liquid can contribute at the most by 0.06 % which is roughly 46% of the total amount. So for window channels liquid water is more important, this is why such channels are used by radiometers to retrive ILW.

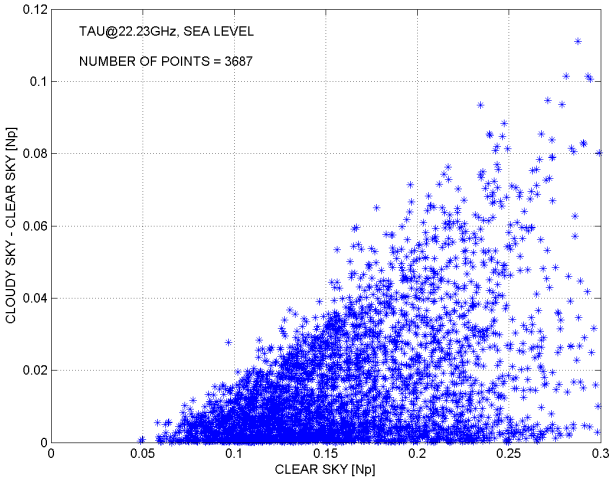

(a)

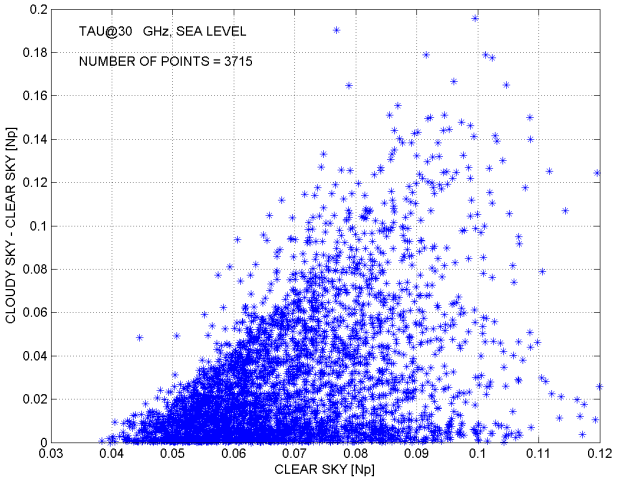

(b)

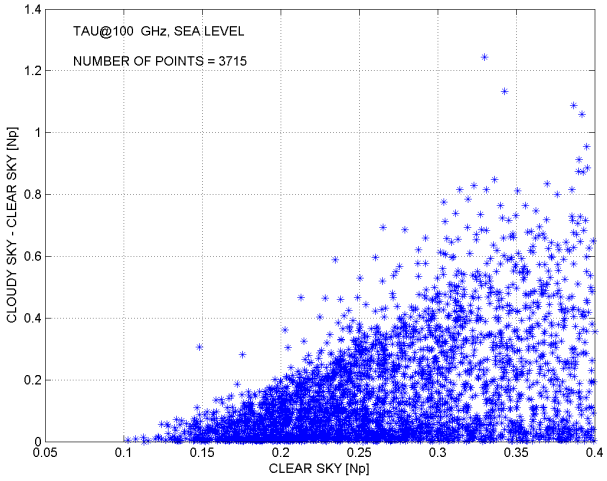

(c)

Figure 7: Difference between opacity values simulated with cloud liquid and without cloud liquid as a function of opacity at 22.23 GHz (b) 30 GHz and (c) 100 GHz.

5.3 Opacity at Different Frequencies

This section shows statistics of atmospheric opacity given in Np for some of the frequencies which the SRT is likely to use. In figure 8 we show low frequency opacity time series obtained by averaging daily values over a 50 year period. Below 20 GHz opacity does not show seasonal behaviour, which means that it is not dependent on weather conditions and vapour content. The 30 GHz frequency is a microwave atmospheric window channel so it too is not highly affected by variations in vapour content during the year. The 30 GHz line is quite correlated to cloud and liquid during the year (fig.6), for this reason it is used by radiometers to retrive ILW. The 22 GHz frequency instead is highly correlated to IWV variations (fig.5). The following results concerning opacity analysis are shown in terms of

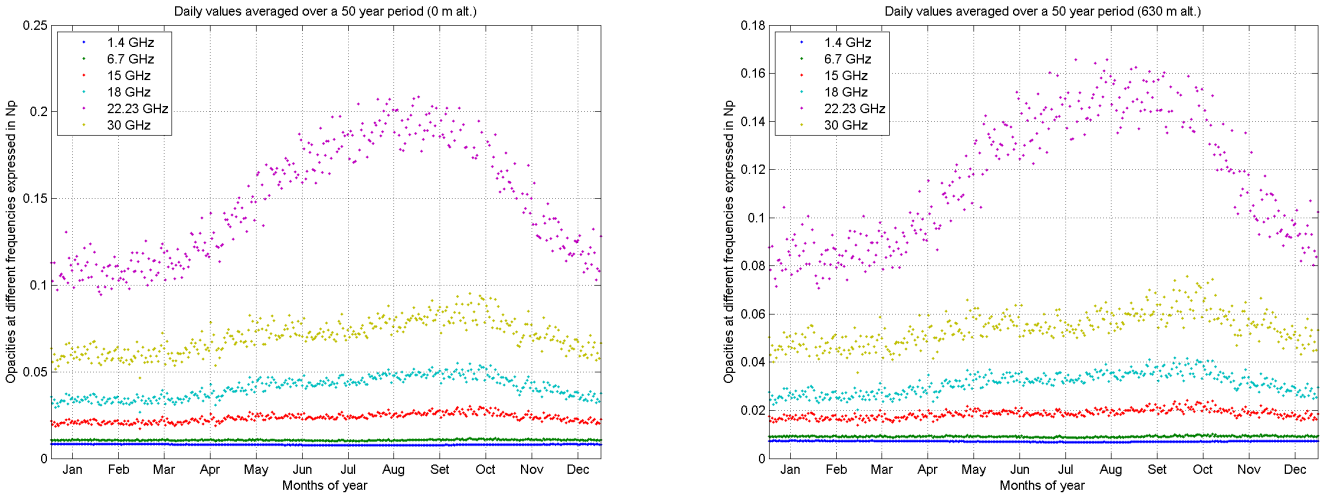

(a) (b)

Figure 8: Daily averaged values of low frequency opacity for (a) sea level (b) SRT altitude.

CDF for some frequencies during different seasons. The results shown in this report and the CDF opacity plots for each month of the year are available on the Web (http://laser3.ca.astro.it/srt). In the following pages, only a few frequencies are shown, the other frequencies can be found in appendix B.

As mentioned in section 2 the 22.23 GHz is an important frequency for SRT and it corresponds to one of the water vapour resonant absorption frequencies therefore the quality of the observation is quite dependent on water vapour content and ultimately on weather conditions. Figure 9 shows the CDF at 22.23 GHz for different seasons, we have plotted both the SRT altitude case (blue line) and the airport altitude case (green line). In the summer there is roughly a 10% chance of having opacity values below 0.1 Np which translated in time periods it means roughly 2 weeks. On the other hand in the Winter there is at least 65% chance of having optimal days for measurements.

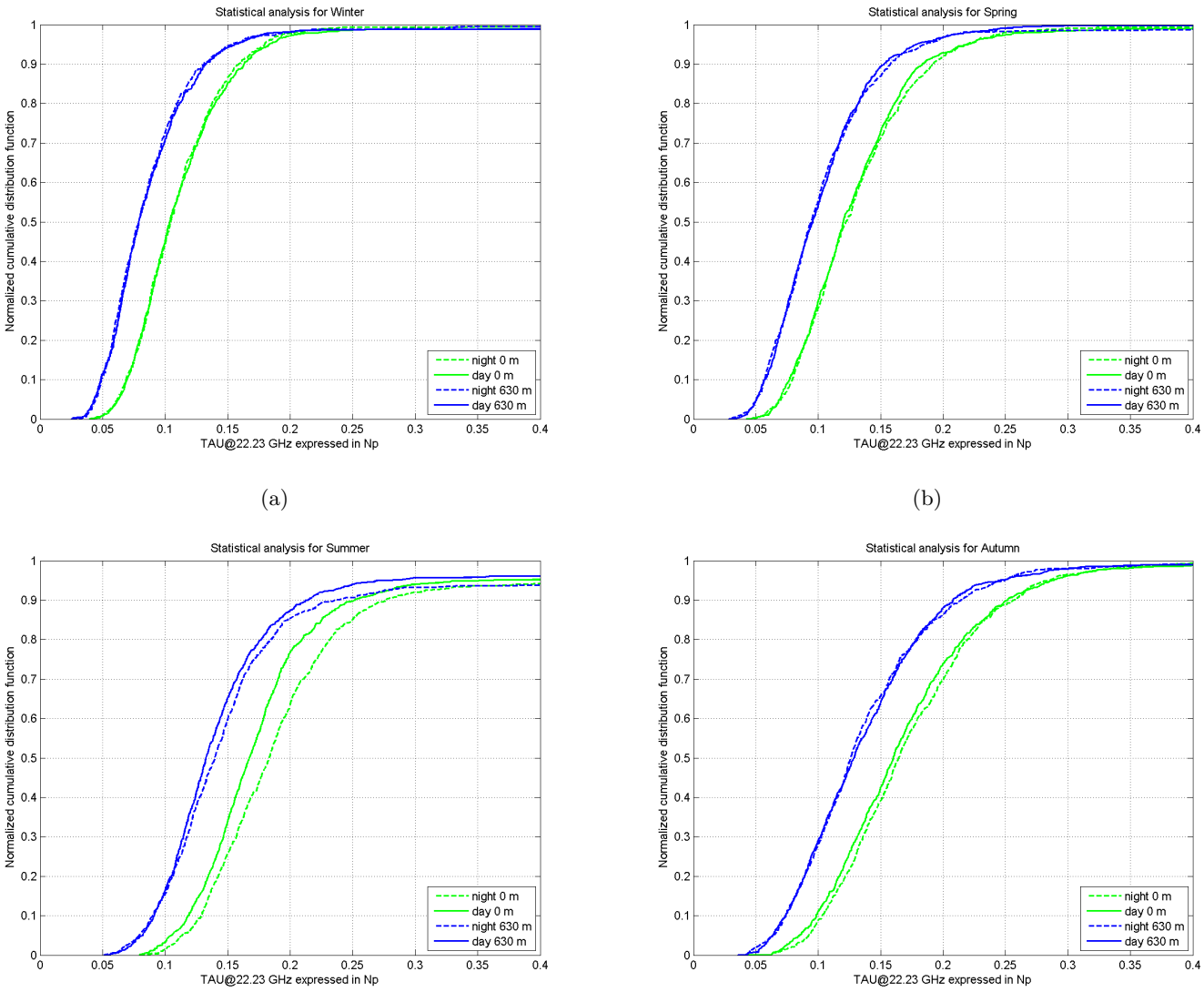

Figure 9: Seasonal opacity cumulative distribution functions at 22.23 GHz.

Very high frequencies such as 100 GHz are useful for measuring CO emissions which in turn are used for H_2 detection. Figure 10 shows seasonal statistics for the 100 GHz frequency. The probability of having good observations is not as good as in the case of lower frequencies. In any case from figure 10 we can deduce that optimal observations will be possible during the winter.

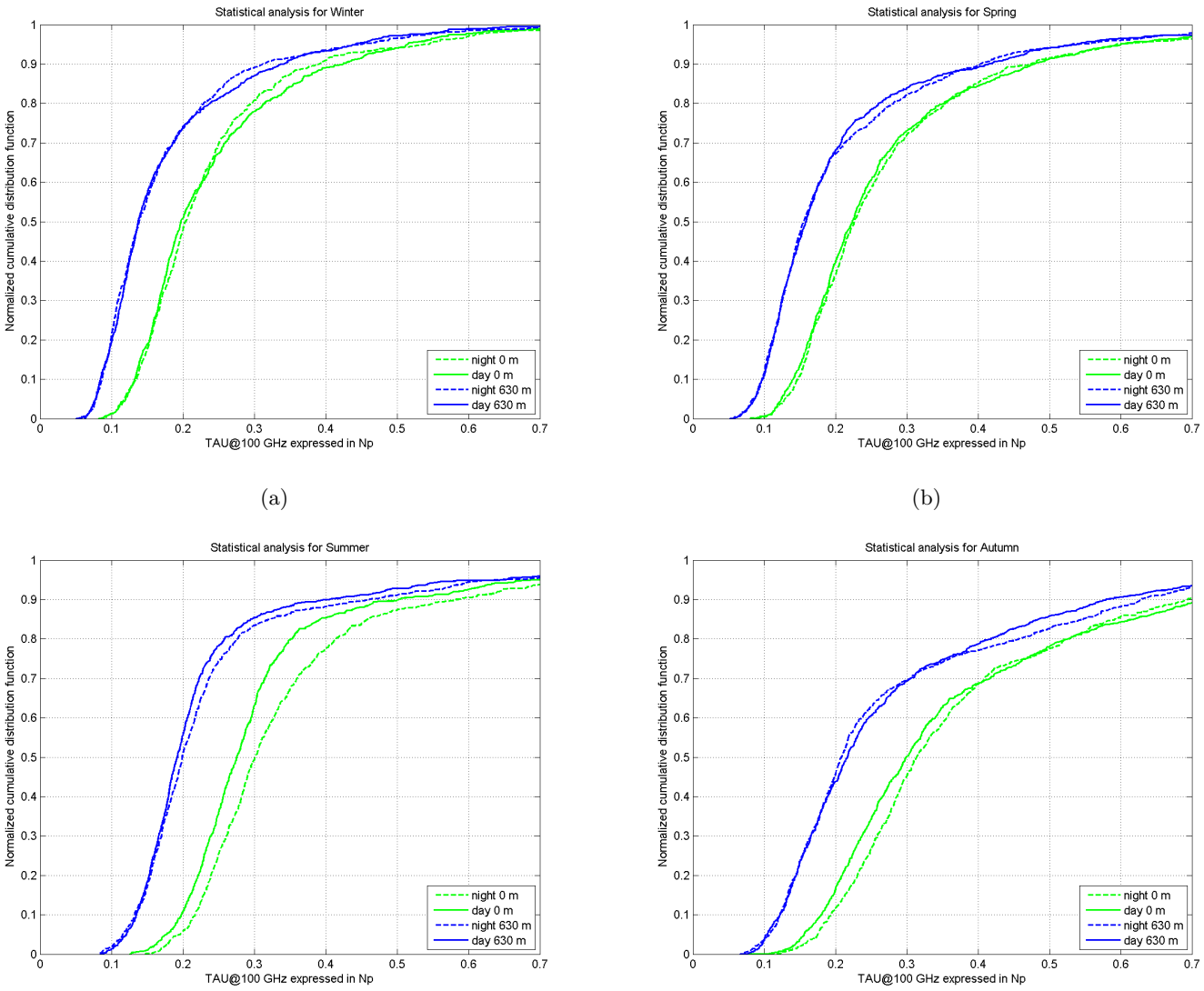

Figure 10: Seasonal opacity cumulative distribution functions at 100 GHz.

The same statistics have been produced for the following frequencies: 22.0, 22.12, 23.698, 23.720, 23.87, 42.821, 43.122, 88.632, 90.664, 110, 115 GHz and they can be found in appendix B.

5.4 Empirical relationships for T_m and T_{mr}

In future we will rely on real time measurements at the SRT site such as GPS and radiometer ones. GPS integrated water vapor measurements are evaluated with equation 16 which requires good T_m estimates. On the other hand opacity can be obtained with equation 10 by using radiometer brightness temperature measurements at different frequencies, this requires good T_{mr} estimates. By using the historical radiosonde dataset we found empirical relationships between T_m and T_s and between T_{mr} and T_s (fig.12 and 11) obtaining monthly statistics of T_m and T_{mr} (table 2).

Month	Tm	Tmr22	Tmr22.12	Tmr22.23	Tmr23.69	Tmr23.72	Tmr23.87	Tmr30
Jan	266.92	266.68	266.07	267.58	267.58	267.55	263.86	270.80
Feb	266.53	266.33	265.69	267.17	267.17	267.14	263.33	270.31
Mar	267.73	267.51	266.80	268.40	268.46	268.46	264.63	271.50
Apr	269.29	269.05	268.33	270.14	270.14	270.13	266.44	272.70
May	273.68	273.33	272.40	274.88	274.88	274.90	271.21	276.88
Jun	277.12	276.55	275.23	278.56	278.56	278.59	274.88	280.13
Jul	280.93	280.93	279.03	282.15	282.16	282.19	278.38	283.65
Aug	281.55	281.17	280.07	282.80	282.81	282.85	279.19	284.32
Sept	278.15	277.85	277.08	279.35	279.35	279.39	276.07	280.88
Oct	275.08	274.92	274.52	276.15	276.15	276.19	273.04	277.74
Nov	271.05	270.91	270.50	271.86	271.87	271.87	268.47	274.16
Dec	268.27	268.11	267.60	268.98	268.99	268.98	265.47	271.71

Table 2: Monthly mean values of T_m and T_{mr} at different frequencies.

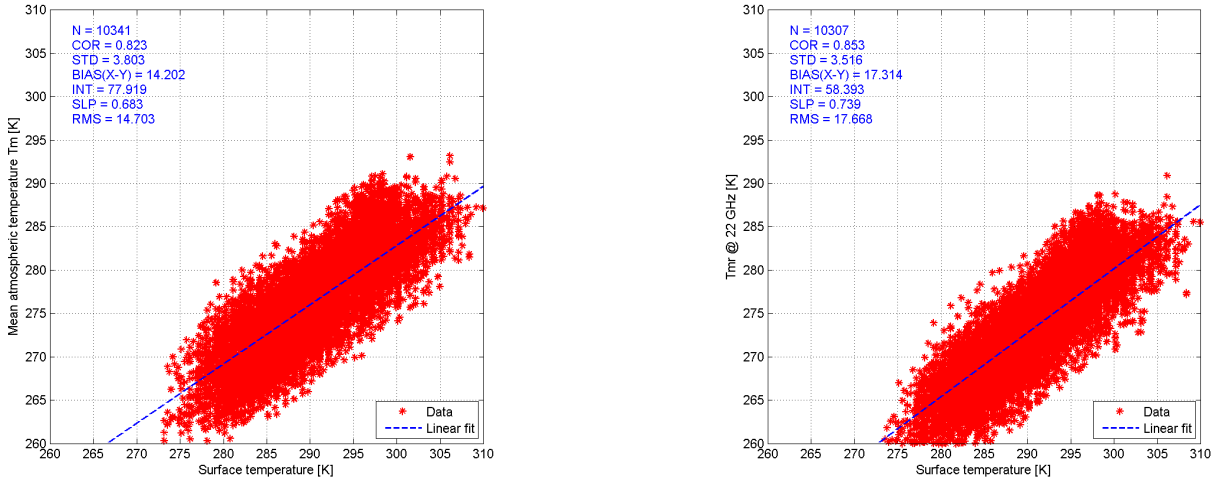

(a) (b)

Figure 11: (a) Mean atmospheric temperature, empirical relationship between T_m and T_s (b) Mean radiative atmospheric temperature, empirical relationship between T_{mr} and T_s.

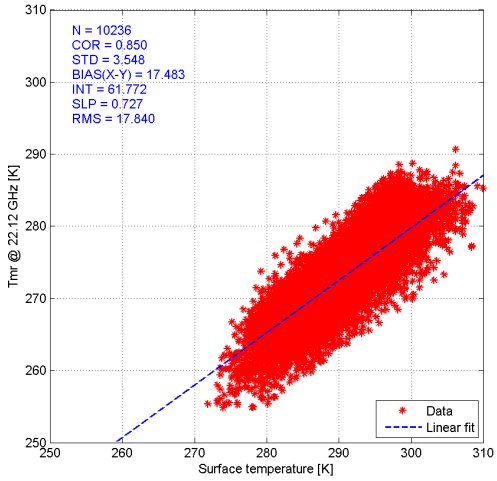

(a)

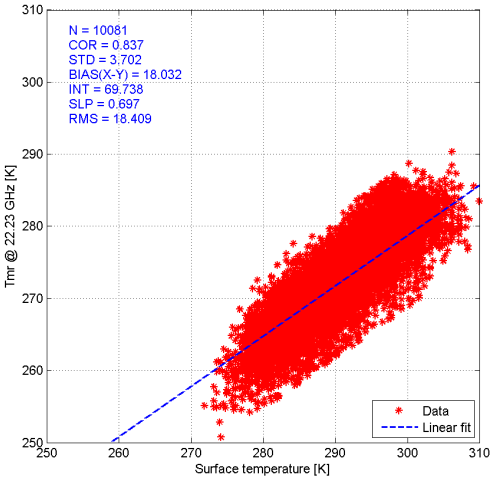

(b)

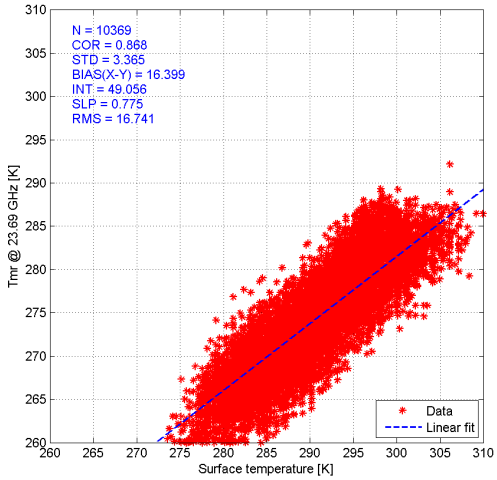

(c)

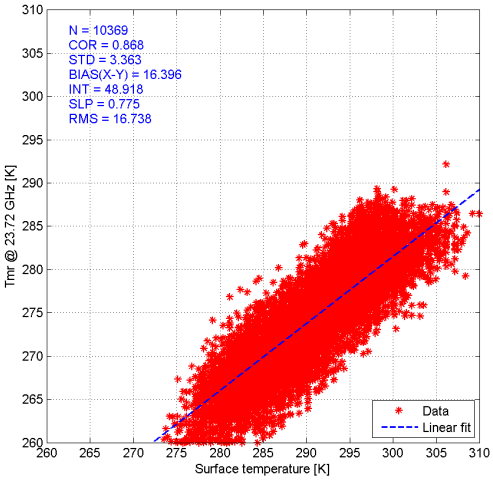

(d)

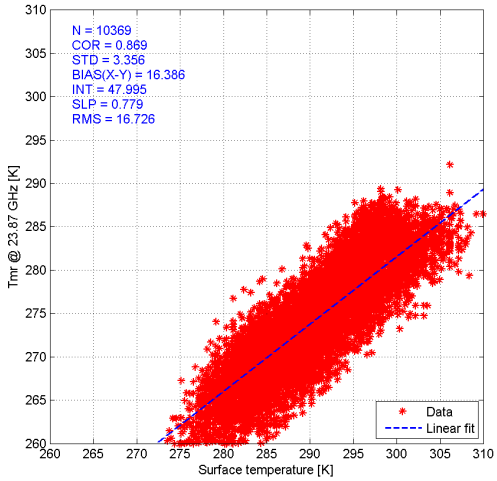

(e)

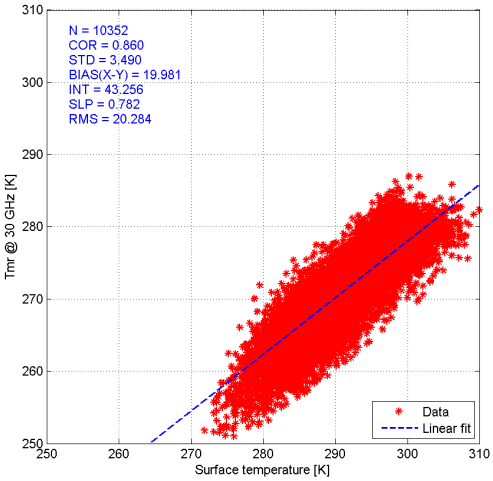

(f)

Figure 12: Mean radiative atmospheric temperature, empirical relationship between T_{mr} and T_s.

5.5 Winds and Profiles

Our statistical analysis is based on radiosoundings performed at Cagliari airport, located at 30 km from the SRT site and at sea level. As we demonstrated in section 5.1, Cagliari airport soundings are representative of the SRT site's atmosphere, nevertheless we have to investigate further how to model the altitude difference between the two sites.
In figure 4 we illustrate something quite interesting: for the airiport site IWV is statistically greater at night time than it is during the day. This tendency is by far more pronounced during summer months and when the lower layers of the atmosphere are considered. Therefore there is a high probability that this phenomenon is restricted to lower layers of the atmosphere (planetary boundary layer) and is more intense when heat exchanges between land, sea and air are greater. To better understand this effect we performed wind statistics obtained from the radiosondes. Statistics take into account intensity and direction, furthermore, by using wind measurements at different epochs we plotted the mean path that a radiosonde launched at Cagliari airport follows during its ascent, figure 13 shows 3-d average wind direction. We can see that at all altitudes (z axis) close to the 300° direction (Mistral)

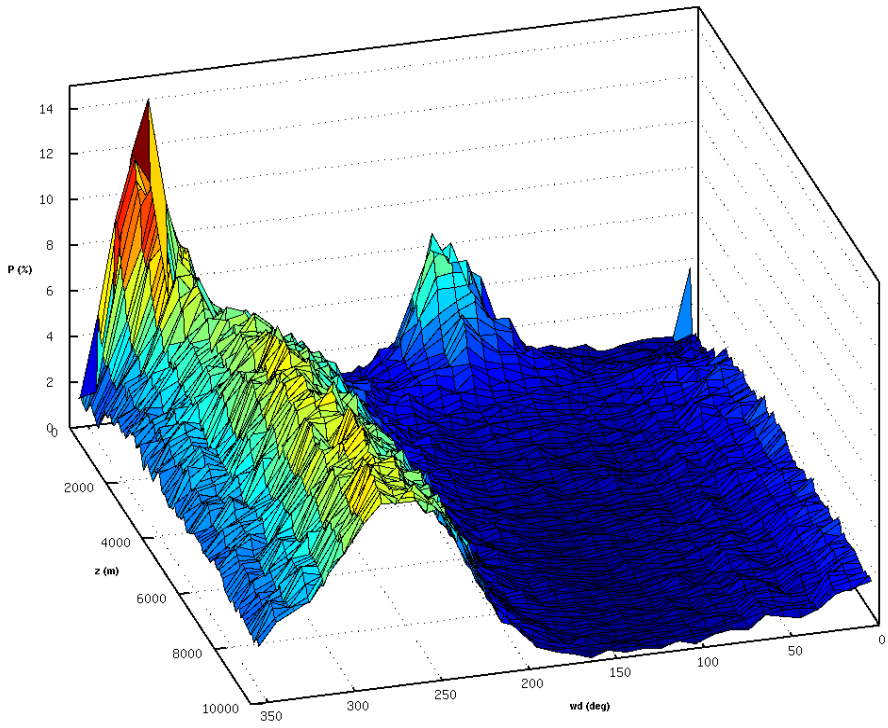

Figure 13: Wind direction probability as a function of height (z) and direction (degrees).

is dominant: when the wind blows over Cagliari there is always a higher probability that it will blow from this direction. Another highly probable wind direction is that close to 150° (Scirocco) especially at sea level. On average most radiosondes are blown towards the South-East direction over the sea.
In figure 13 we can see how average wind speed increases with height as would be expected from thermal wind balance (Holton, 2004). At roughly 5-7 m/s (18-25 km/h) radiosondes are rapidly blown over a water surface: firstly above the Santa Gilla lagoon and then directly above the sea, figure 15 shows the average radiosonde path. Probably the reason why during the summer IWV at low altitudes over water surfaces is higher at night time than day time is due to higher water-air temperature gradients which drive stronger evaporation.

Finally we show (fig.16) mean relative humidity profiles during the day time and during the night

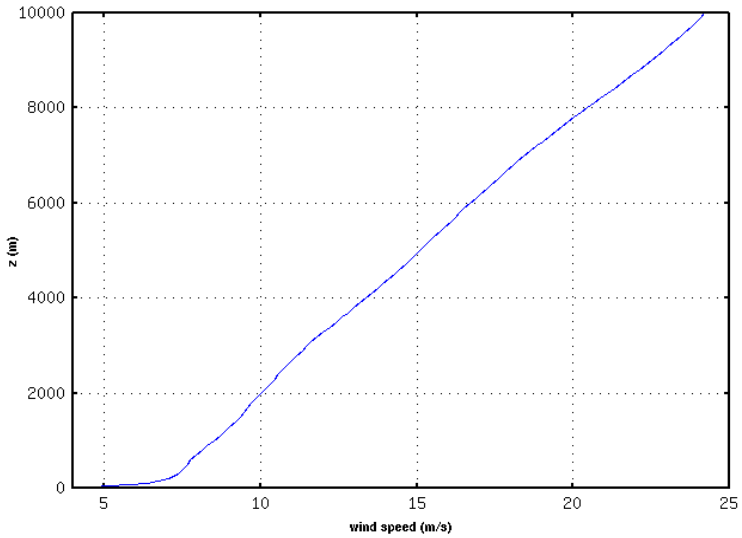

Figure 14: Wind speed as a function of height.

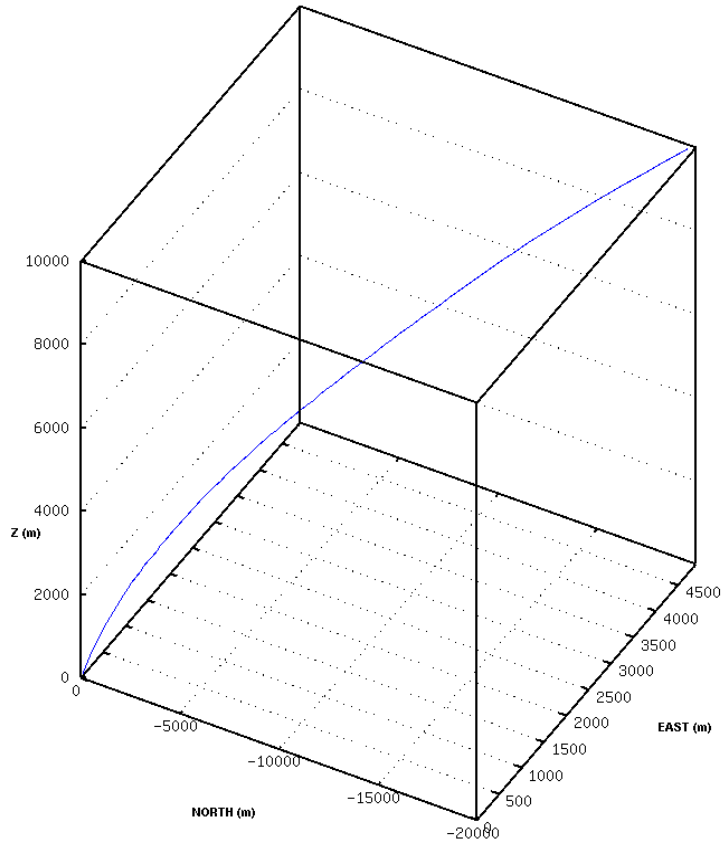

Figure 15: Radiosonde mean trajectory above Cagliari.

time considering each time 3 different cases: low IWV ($< 10\ mm$) average relative humidity profile, high IWV ($> 10\ mm$) average relative humidity profile and average profile using all measurements indistinctly. Considering different cases is useful because one can see typical relative humidity profiles under specific circumstances (eg. very humid conditions, dry conditions). As can be seen from figure

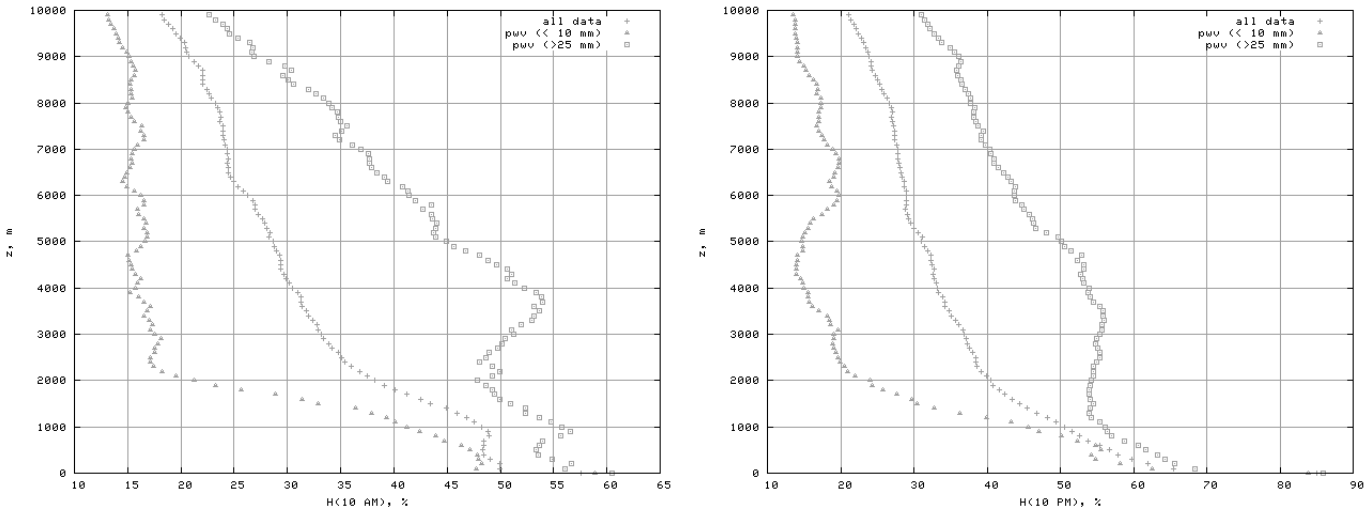

(a) (b)

Figure 16: Relative humidity profiles (a) during the day time (b) during the night time.

16, 22 UTC relative humidity profiles are systematically higher than 10 UTC ones, this is true especially within the boundary layer and it is consistent with the results of section 5.2. Studying mean profiles and associating them to particular weather configurations (eg. fronts, humidity, winds) could be useful in future to implement particular nowcasting schemes in order to predict favorable conditions for radio-astronomical observations.

6 Conclusions

In the present report we provide an overall view of some of the key geophysical quantities that influence the quality of radio astronomical observations at the Sardinia Radio Telescope (SRT) site. In particular, we investigate the following quantities: integrated water vapor content (IWV) and opacity at different frequencies, integrated liquid water content (ILW), mean temperatures and wind occurence. These elements are analysed in a statistical sense, deriving average values and determining their variations during the year. In addition, we introduced our future goals and aims in the framework of the climatic/geophysical characterization of the SRT site: i) real time radiometer and geodetic GPS (Global Positioning System) receiver measurements; ii) short range forecasting of some of the aforementioned geophysical quantities.
Our results can be summarized as follows:

- the Cagliari airport historical radiosonde dataset (1950-2007) is representative of the SRT site atmosphere, therefore it represents a useful tool for the site's characterization. Further investigations are instead needed to model the altitude difference between the airport site and the SRT one and will be addressed in a future work.

- Mean annual time series show that during winter months IWV content is usually less than 10 mm, while during summer ones it is tipically less than 20 mm. We also showed IWV statistics in terms of cumulative distribution function (CDF) during seasons. Integrated liquid water varies on average from 0-0.2 mm during winter months to 0-0.8 mm during summer ones. The cloud coverage is also higher during autumn and winter, nevertheless, for resonant frequencies, liquid water absorption is usually less than that due to water vapor.

- CDF statistics of atmospheric opacity performed at different frequencies indicate that, during winter months, there is a 60% probability (about 17 days per month) of obtaining observations at 22 GHz (e.g. water maser lines) characterized by an opacity lower than 0.1 Np. For the same opacity treshold, the probability goes down to about 10% during the summer period. Concerning the frequency range around 100 GHz (that includes for example the carbon monoxide, CO, main transitions), indications exist that SRT observations, characterized by an opacity lower than 0.1-0.15 Np, are possible during winter, although for a limited number of days (about 6 days a month).

- Empirical relationships of the mean atmospheric and radiative temperatures were obtained by using the historical time series. These information permit to obtain the IWV and atmospheric opacity with the use of the GPS receiver and the radiometer, respectively .

- Wind statistics and the radiosondes mean path were studied. This analysis is particularly relevant to understand how to deal with radiosonde measurements obtained in a site that is not perfectly co-located with the one under analysis.

Next steps of our activity imply to further improve the present analysis through additional measurements performed with a radiometer and a geodetic GPS receiver recently installed at the SRT site.

Acknowledgements

The authors are grateful to Dr. Andrea Tarchi for his useful suggestions regarding the report and to Dr. Mauro Sorgente for his contributions to the data processing of the GPS receiver.

References

Bevis M., Businger S., Chiswell S., Herring T., Anthes R., Richard A., Rocken C., Ware R. H., 1994: "GPS Meteorology: Mapping Zenith Wet Delays onto Precipitable Water". *Journal of Applied Meteorology*, Vol. 33, pp. 379-386.

Buehler S. A., Eriksson P., Kuhn T., Von Eneln A. and Verdes C., 2005: "ARTS, the Atmospheric Radiative Transfer Simultor". *J. Quant. Spectrosc. Radiat. Transfer*, Vol. 91(1), pp. 65-93.

Cimini D., Westwater E., R., Gasiewski A. J., Klein M., Leuski V., Y. and Liljegren J. C., 2007: 'Ground-Based Millimeter and Submillimeter-Wave Observations of Low Vapor and Liquid Water Contents". *IEEE Transaction on Geoscience and Remote Sensing*, Vol. 45, N. 7, pp. 2169-2179.

Cimini D., Nasir F., Westwater E. R., Paine V. H., Turner D. D., Mlawer E. J., Exner M. L., and Cadeddu M. P., 2009: "Comparison of Ground-Based Millimeter-Wave Observations and Simulations in the Artic Winter". *IEEE Transaction on Geoscience and Remote Sensing*, Vol. 47, N. 9, pp. 3098-3106.

Memmo A., Fionda E., Paolucci T., Cimini D., Ferretti R., Bonafoni S. and Ciotti P., 2005: "Comparison of MM5 Integrated Water Vapor With Miceowave Radiometer, GPS, and Radiosonde Measurements". *IEEE Transaction on Geoscience and Remote Sensing*, Vol. 43, N. 5, pp. 1050-1058.

Mendes V. B., Prates D., Santos L., Langley R. B., 2000: "An Evaluation of Models for the Determination of Mean Weighed Temperature of the Atmosphere". *Proc. of the 2000 National Technical Meeting. Institute of Navigation*, USA, pp. 443-439, 2000.

Pacione R., Lanotte R., Fionda E., Ferrara R., Sciaretta C., Vespe F., Mureddu L., 2002: "Comparison of Atmospheric Parameters Derived from GPS, VLBI and Ground-Based Microwave Radiometer over Italy. *Physical and Chemestry of the Earth, Parts A/B/C*, Vol. 27, Issues 4-5, pp. 309-316.

Petty G. W., 2006: "A First Course In Atmospheric Radiation". Second Edition, Sundog Publishing, Printed in the United States of America.

Pulvirenti L., Pierdicca N., Marzano F. S., 2005: "Simulating Brightness Temperatures in Cloudy Conditions Over the Mediterranean Sea". *Proc. of URSI GA 2005*, New Delhi.

Holton J. R., 2004: "An Introduction to Dynamic Meteorology", Fourth Edition, Elsevier Academic Press, Printed in the United States of America.

Janssen M., A., 1992: "Atmospheric Remote sensing by Microwave Radiometry". Wiley series in remote sensing, Printed in United States of America.

Kirkpatrick S., Gelatt C. D. and Vecchi M. P., 1983: "Optimization by Simulated Annealing". *SCIENCE*, Vol. 220, N. 4598, pp. 671-679.

Rodgers C. D., 2000: "Inverse Methods for Atmospheric Sounding: Theory and Practice". World Scientific Publishing Company, London, UK.

Sandri M. and Ambrosini R., 1999: "Probabilità Cumulative e Serie Temporali di Opacità con Radiometro WVR da Cagliari per L'Anno 1999". *IRA Internal Report*, IRA 296/00.

Turner D. D., Clough A. S., Liljegren J. C., Clothiaux E. E., Cady-Pereira K. E., Gaustad K. L., 2007: "Retriving Liquid Water Path and Precipitable Water Vapor From the Atmopsheric Radiation Measurements (ARM) Microwave Radiometers". *IEEE Transaction on Geoscience and Remote Sensing*, Vol. 45, N. 11, pp. 3680-3690.

Turner D. D., Vogelmann A. M., Austin R. T., Barnard J. C., Cady-Pereira K. E., Chiu J. C., Clough S. A., Flynn C., Kahiyer, M. M., Liljegren J., Johnson K., Lin B., Cady-Pereira K. E., Long B., Marshak A., Matrosov S. Y., McFarlane S. A., Miller M., Min Q., Minnis P., O'Hirok W., Wang Z. and Wiscombe W., 2007: "Thin Liquid Water Clouds, Their Importance and Our Challange". *Bull. Amer. Meteor. Soc*, pp. 177-190.

S. Wu, 1979: "Optimum Frequencies of a Passive Microwave Radiometer for Tropospheric Path-Length Correction". *IEEE Transactions on Antennas and Propagation*, Vol. AP-27, N. 2, pp. 233-239.